

Characterization of deep defects responsible for the quenching behavior in undoped GaN layers

H. Witte,* E. Schrenk, K. Flügge, A. Krost, and J. Christen

Otto-von-Guericke-University Magdeburg, Institute of Experimental Physics, 39016 Magdeburg, Germany

B. Kuhn and F. Scholz†

4. Physikalisches Institut, Universität Stuttgart, 70550 Stuttgart, Germany

(Received 26 July 2004; revised manuscript received 21 September 2004; published 30 March 2005)

In undoped semi-insulating GaN samples grown by metal-organic vapor phase epitaxy on sapphire, the recombination and quenching processes were investigated for the main deep traps responsible for quenching. A comprehensive picture is obtained by using different complementary techniques of thermally stimulated current spectroscopy (TSC). Three traps— $Q1$, $Q2$, and $Q3$ —were separated in the temperature region between 200 and 300 K. Variations of the excitation and the cleaning temperature suggest a two-step trapping process of the defects $Q2$ and $Q3$. Quenching experiments evidence the involvement of these traps in the quenching process and the existence of two metastable states. These results are summarized in a model involving two metastable states and a complex two-step recharging trapping process.

DOI: 10.1103/PhysRevB.71.125213

PACS number(s): 71.55.Eq, 73.50.Gr, 73.61.Ey

I. INTRODUCTION

GaN is a well-established material in devices such as blue laser diodes or high-frequency and high-temperature transistors. In these applications, important parameters such as the free-carrier concentration, the recombination rates, or the frequency response are strongly influenced by deep point defects. In particular, recharging effects of metastable or multiple charged states create persistence or quenching phenomena of important device parameters.¹ Therefore, knowledge and understanding of the dynamics of traps is crucial. We, and others, investigated the trapping kinetics of some of these traps as well as the quenching phenomena caused in semi-insulating undoped GaN layers using the technique of thermally stimulated current (TSC).^{2–4} Nevertheless, the traps involved in the quenching process have not been analyzed in detail up to now. In this work, we succeeded in isolating and characterizing the defects involved in these processes using different complementary techniques of TSC. We present a comprehensive model for the complex recharging mechanism.

II. EXPERIMENT

All samples were grown by metal-organic vapor phase epitaxy on (0001) sapphire substrates with an optimized AlN seed layer and are nominally identical. They are all semi-insulating having a specific resistivity of above $10^4 \Omega \text{ cm}$ (samples no. 1, no. 2, and no. 3) and photoluminescence linewidths below 3 meV at 4.2 K. Because of their slightly different quenching behavior, they are numbered no. 1, no. 2, and no. 3.

dc-sputtered and consecutively annealed Al layers and dc-sputtered Pt layers were used as contacts in coplanar arrangement.

Deep defects were investigated by TSC using different excitations schemes. In conventional TSC, the sample is excited at 80 K by a low-pressure Hg lamp with a short pass

filter at 335 nm (known as uv excitation—above-band-gap light) and subsequently heated up to 450 K (see Table I conventional procedure). For the separation of different trap emissions resulting in superposed TSC peaks, we used a cleaning procedure as described in Ref. 5 consisting of the following steps: uv excitation at 80 K to photocurrent saturation, heating up to a temperature T_{ann} near the peak maximum of the trap emission of interest, subsequent cooling down to 80 K, and heating up once more to 450 K but without optical excitation (see Table I, cleaning procedure). To investigate the trapping kinetics, a second excitation for 30 s at a defined temperature (T_{exc}) was realized with uv light. This second excitation scheme consists of the following steps: uv excitation at 80 K to photocurrent saturation, heating up to T_{exc} ; second uv excitation, fast cooling down back to 80 K, and heating up to 450 K without illumination (see Table I, second excitation uv). In this way, we get information on whether and how high-temperature thermal emissions are influenced by the draining of low-temperature traps. Simultaneously, the activation energy can be determined by the initial rise method described in Ref. 5 if the TSC peaks are thermally cleaned from other superposed emissions at the low-temperature side (described as fractional TSC in Ref. 6). The heating rate was constant at 0.18 K/s in all procedures.

For quenching experiments, the samples were excited by the uv lamp and a subsequent illumination with a 690 nm laser diode (below-band-gap light at 1.8 eV) for 3 min at the same temperature of 80 K followed by a conventional heating up to 450 K (see Table I, quenching procedure). Furthermore, a second excitation with a 675 nm laser diode was applied at variable temperatures T_{exc} as described above (see Table I, second excitation quenching). The thermal activation energies E_a of the TSC traps were determined by several methods. The initial rise method uses the slope of the peak versus $1/kT$, whereas in the heating rate method the activation energy is obtained from the Arrhenius plot $\ln(T_m^4/\beta)$ versus $1/kT_m$ assuming a monomolecular recombination.

TABLE I. Steps in TSC spectroscopic procedures (for details, see text).

| Step | Excitation | Heating up | Second excitation at T_{exc} | Fast cooling down | Heating up |
|--------------------------------|------------------|---------------------|------------------------------------------|----------------------|------------|
| Conventional TSC | uv | | | | to 450 K |
| Quenching | uv and 690 nm | | | | to 450 K |
| Cleaning | uv | to T_{ann} | | to 80 K | to 450 K |
| Second uv excitation | uv | to T_{exc} | with uv | to 80 K | to 450 K |
| Second quenching excitation | uv | to T_{exc} | with 690 nm | to 80 K | to 450 K |

The peak position method uses the relation $T_m^4/\beta \sim \exp(E_a/kT_m)$ and needs only a conventional TSC spectrum. All methods are discussed in detail in Ref. 5.

III. RESULTS AND DISCUSSION

In Fig. 1, an unquenched and a quenched TSC spectrum of the SI sample no. 1 are shown. In the unquenched TSC spectrum, we can distinguish four different regions of thermal emissions. Region $T1$ between 80 and 120 K is characterized by thermal emissions with activation energies below 200 meV (described in Refs. 2 and 4 in detail). A broadband $T2$ follows it between 120 and 200 K that corresponds to emissions with activation energies between 0.23 and 0.32 eV as reported in Ref. 7. In the thermal region $T3$, all trap emissions are superimposed and broadbands are observed. In this range $T3$, several traps were observed in Ref. 8 with activation energies at 0.45 and 0.56 eV. At about 300 K, the TSC signal decreases followed by the region $T4$, where the signal rises again indicating further traps.

The quenched spectrum in Fig. 1 was obtained by using a further excitation at 80 K with below-band-gap light (red light at 675 nm=1.8 eV), which generates a decrease of the peak heights in the whole TSC spectrum. The most remarkable quenching is observed in the temperature region $T3$ (described also in Ref. 2). Therefore, in the following, this region will be investigated in detail.

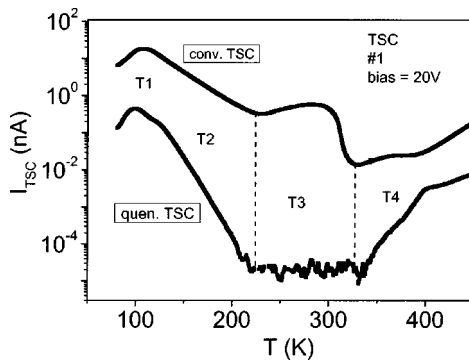


FIG. 1. TSC spectra excited at 80 K with 325 nm UV light (conventional TSC) to the saturation of photocurrent and additionally illuminated with a 690 nm laser (quenched TSC) of the semi-insulating, undoped GaN sample no. 1. The heating rate was 0.18 K/s.

A. Peak separation by cleaning procedure and trap kinetics in the $T3$ region

One problem is the superposition of various peaks. For separation, the peaks were cleaned by heating up to a temperature T_{ann} between 200 and 275 K (cleaning procedure) as shown in Fig. 2 (left). In this way, the low-energy traps were drained and the interesting peaks could be observed without interference. Three peaks labeled as $Q1$ at 215 K, $Q2$ at 255 K, and $Q3$ at 290 K (Fig. 2, right) can now be distinguished. Under these conditions, the peak heights of emissions $Q2$ and $Q3$ increase with increasing T_{ann} between 80 and 250 K. These emissions were further investigated by the second excitation procedure with the uv lamp (above-band-gap light, 30 s) at $170 \text{ K} < T_{\text{exc}} < 225 \text{ K}$ to support the separation of the peaks. This effect is shown in Fig. 3 (left) for the SI sample no. 2 for different temperatures T_{exc} . As in the cleaned spectra of Fig. 2, an increase of the $Q2$ and $Q3$ peak heights with increasing excitation temperature T_{exc} is obtained, which show similar behavior to the main traps in Refs. 9 and 10 where a second excitation procedure and an excitation at different temperatures were used, respectively. Furthermore, the peak heights of $Q2$ and $Q3$ change differently with annealing and excitation temperatures. Therefore, the ratio between the peak heights of $Q2$ (at 270 K) and $Q3$ (at 290 K), defined as $Q2/3$, is determined for the different cleaning temperatures and normalized to $Q2/3$ excited at 80 K. This ratio $Q2/3(T_{\text{ann}})/Q2/3(80 \text{ K})$ is plotted in Fig. 3

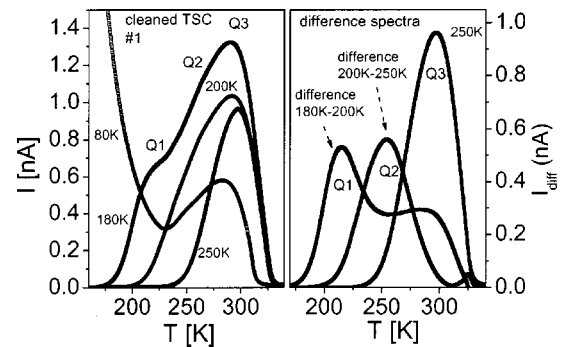


FIG. 2. Cleaned TSC spectra in region $T3$ at 80, 175, and 225 K for sample no. 1 shown in Fig. 1 (left). Difference spectra between the TSC curves annealed at 180, 200, 200, and 250 K and the cleaned TSC spectrum at 250 K. The separated peaks are clearly seen (right).

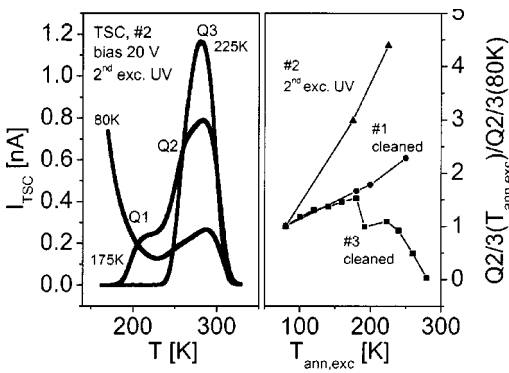


FIG. 3. TSC spectra of sample no. 2 using a second excitation with the UV light (above band gap) at different excitation temperatures (T_{exc}) (left). Peak height ratio between $Q2$ and $Q3$ ($Q2/3$) at different T_{ann} and T_{exc} normalized to $Q2/3$ at 80 K vs the cleaning and the excitation temperatures (right).

(right) as a function of T_{ann} . This ratio increases between 100 and 270 K and decreases above 270 K (emptying of trap $Q3$). As can be seen in Fig. 3 (right), the $Q3$ peak height increases due to the second excitation with uv light showing a nonsaturation of the trap $Q3$.

This behavior can only be explained by complex recombination kinetics. Similar effects of the second excitation procedure were observed for photoexcited TSC in $Bi_{12}SiO_{20}$.⁹ Similarly, our observations can be understood in terms of a charge-transfer model as shown in Fig. 4 (left). The emptying of the low-temperature traps induces a charge transfer from traps involved in $T1$ and $T2$, e.g., into the trap $Q2$. As a consequence, the probability of the direct thermal transition of carriers from a band into a deep trap is lower than that via shallower traps. These transfer processes also explain the dependence of the peak heights of the cleaning temperature. The traps $Q2$ and $Q3$ should be only partially filled by the uv excitation at 80 K. If the shallower traps are emptied by the cleaning process (heating up to T_{ann} below the emission of $Q2$), charges from these shallower defects are slowly captured by deeper traps. In this way, the filling rates and thereby the peak heights of $Q2$ and $Q3$ increase due to the emptying of the shallower traps (Fig. 4). This transfer process must be time-dependent and slow,

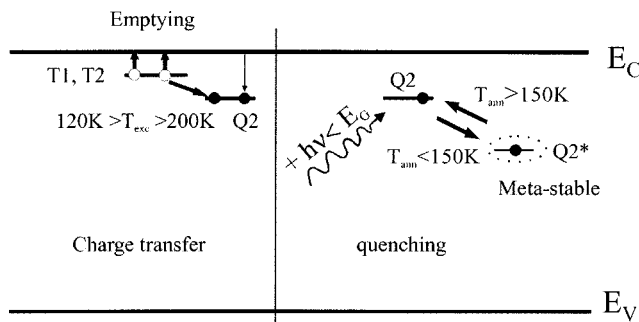


FIG. 4. Charge-transfer model for explanation of the peak height increase induced by varying excitation temperatures $T_{exc} > 200$ K for the example of $Q2$ (left). Scheme of the transfer of the example $Q2$ trap into the corresponding metastable state $Q2^*$ induced by below-band-gap quenching illumination ($h\nu < E_G$) (right).

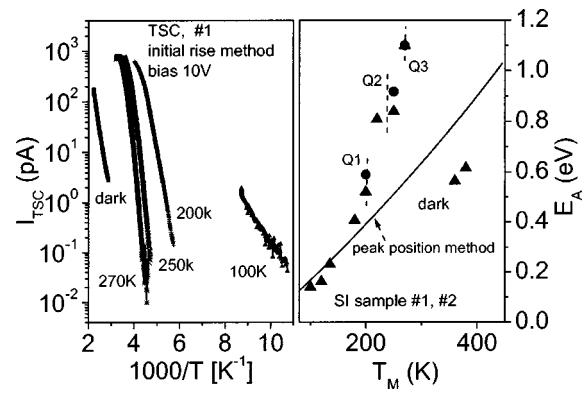


FIG. 5. Arrhenius plots of initial rises of TSC emissions of sample no. 1 after fractional heating procedure (left) and the dependence of activation energies used the initial rise method on the annealing temperature of samples no. 1 and no. 2 (right). The activation energies as determined by the peak position method are representing by the line. All dark values were determined from TSC curves without any excitation.

since the conventional TSC procedure shows lower peak heights.

The activation energies of the traps $Q2$ and $Q3$ were commonly determined using the initial rise method and the heating rate method. The heating rate method yields values in a wide range between 0.25 and 0.5 eV for both peaks $Q2$ and $Q3$. The values obtained from this method strongly differ from sample to sample and, furthermore, depend on the number of Gaussians used (two or three) for the separation of the superposed peaks. This behavior indicates a nonconstant recombination lifetime or a bimolecular kinetic, as is described in Ref. 12. For this kinetic, the heating rate method is not adequate for the determination of the real activation energy. In contrast, the initial rise time method does not depend on the specific recombination process, as has been shown in Refs. 5 and 12. Therefore, the activation energies of $Q2$ and $Q3$ determined from the initial rise time method were considered for further interpretations. The corresponding Arrhenius plots are shown in Fig. 5 (left) and yield activation energies in the range from 0.8 to 1.1 eV for $200\text{ K} < T_{ann} < 300\text{ K}$ which are very high as compared to those above 300 K (see Fig. 5, right). In Ref. 8, activation energies between 0.4 and 0.65 eV were given for these TSC emissions, which are similar to those determined with the peak position method (Fig. 5, right). Furthermore, in Ref. 13, using the photoinduced transient current spectroscopy, three emissions are described at 250, 280, and 350 K with 0.4 (electron trap), 0.85 (hole trap), and 1.1 eV (electron trap), respectively. The traps at 0.85 and 1.1 eV are very similar to the initial rise values of $Q2$ and $Q3$, whereby the varying peak positions can be caused by the different measurement methods. Because the peak position method and the heat rate methods need the same assumptions (monomolecular kinetics), the activation energies determined with the initial rise method should be more realistic with respect to the complex trapping kinetics in the emission region $T3$.

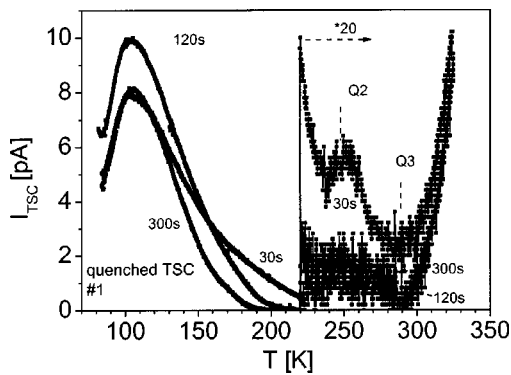


FIG. 6. Quenched TSC spectra of sample no. 1 excited with 690 nm laser light for different illumination times. For times longer than 120 s, the emissions $Q2$ and $Q3$ are fully quenched.

B. Quenching effects

In Fig. 6, the quenching of region $T3$ for different illumination times with the 690 nm laser light is shown. For times above 120 s, the peak $Q2$ vanishes, whereas this emission is observed for shorter times showing the quenching process being saturated and, therefore, depending on the recharging of defined concentrations of the traps $Q2$ and $Q3$. The quenching of $Q2$ and $Q3$ drastically depends on the temperature T_{exc} during the second excitation with quenching laser light as shown in Fig. 7. Three different effects are distinguished.

(i) The peak $Q2$ is fully quenched at 80 K and reappears at excitation temperatures above 100 K (Fig. 7, left). The thermal recovery suggests that this quenching is controlled by thermal emissions up to 100 K. Similar effects are described in Ref. 11 for GaAs.

(ii) At higher excitation temperatures ($200\text{ K} < T_{exc} < 250\text{ K}$), the peak height of $Q3$ increases up to a factor 3, whereas the peak $Q2$ rapidly decreases, i.e., the recovery temperature of the $Q3$ quenching is connected to the emission of $Q2$, indicating a correlation between $Q2$ and $Q3$ within the quenching process. The recovery of quenching at temperatures of about 100 and 200 K indicate the existence of two metastable states $Q2^*$ and $Q3^*$ comparable to thermal quenching phenomena in GaAs in Ref. 11. These metastable defects are excited trap states, which interact with none of the bands having an energetic barrier to their ground states (see Fig. 4, right). Otherwise, the peak height enhancement

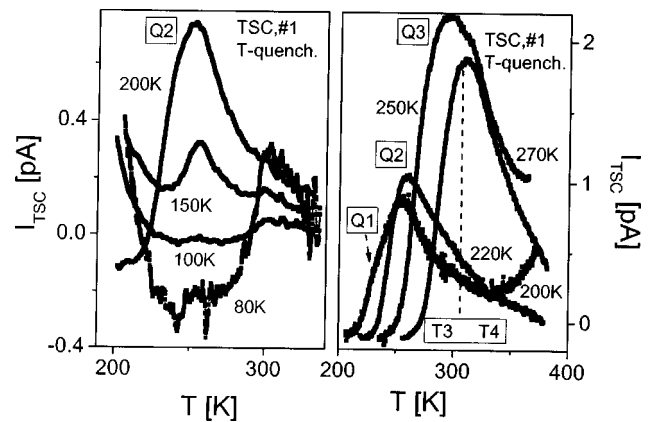


FIG. 7. TSC spectra between 200 and 400 K of sample no. 1 using the second excitation with quenching light (see the procedure in Table I). The 690 nm illumination times are 120 s (left) and 30 s (right).

of $Q2$ and $Q3$ gives rise to the assumption of a two-step capture process of $Q2$ and $Q3$ via shallower traps (charge-transfer process, Fig. 4, left) as discussed above.

(iii) At $T_{exc} > 250\text{ K}$, thermal emissions in the region $T4$ above 320 K are enhanced, as compared to those in the uv-excited and in the TSC spectra quenched at lower temperatures. In contrast to the recovery of the quenching of $Q2$ and $Q3$, the emissions in $T4$ are suppressed under normal excitation conditions. In all cases, the peak heights in $T3$ and $T4$ increase with increasing temperature of the second quenching excitation.

IV. SUMMARY

In summary, we investigated the recombination and quenching kinetics of traps in SI-GaN between 200 and 300 K. Three peaks $Q1$, $Q2$, and $Q3$ at 215, 268, and 291 K, respectively, were separated and characterized in detail by cleaning processes and variations of the time and the temperature of an additional uv illumination. In quenching experiments by variation of the temperature of the second red illumination, two recovery temperatures of quenching phenomena at about 100 and 200 K were observed, as was a further increase of the peak height with increasing temperature T_{exc} , indicating the existence of two metastable states as well as a complex two-step recharging process. These results are integrated in a model including two metastable states and a complex two-step recharging process.

*Email address: hartmut.witte@physik.uni-magdeburg.de

[†]Present address: Ulm University, Dept. Optoelectronics, 89081 Ulm, Germany.

¹P. B. Klein, S. C. Binari, J. A. Freitas, and A. E. Wickenden, *J. Appl. Phys.* **88**, 2843 (2000).

²H. Witte, A. Krtischil, M. Lisker, E. Schrenk, J. Christen, A. Krost, B. Kuhn, and F. Scholz, *Appl. Phys. Lett.* **82**, 4083 (2003).

³Z. Q. Fang, B. B. Claffin, D. C. Look, T. M. Myers, D. D.

Koleske, A. E. Wickenden, and R. L. Henry, in *GaN and Related Alloys*, edited by C. Wetzel, E. T. Yu, J. S. Speck, A. Rizzi, and Y. Arakawa, MRS Symposia Proceedings No. 743 (Materials Research Society, Pittsburgh, 2002), Vol. 743, p. L11.33.

⁴U. V. Desnica, M. Pavlovic, Z. Q. Fang, and D. C. Look, *J. Appl. Phys.* **92**, 4126 (2002).

⁵D. V. Desnica, *J. Electron. Mater.* **21**, 463 (1992).

⁶R. Fasbender, G. Hirt, M. Thoms, and A. Wickacker, *Semicond. Sci. Technol.* **11**, 935 (1996).

- ⁷W. H. Jung, T. W. Kang, T. W. Kim, and K. S. Chung, *Jpn. J. Appl. Phys., Part 2* **39**, L1084 (2000).
- ⁸W. H. Jung, T. W. Kang, and T. W. Kim, *Jpn. J. Appl. Phys., Part 2* **41**, L509 (2002).
- ⁹T. Takamori, *J. Appl. Phys.* **69**, 8222 (1991).
- ¹⁰H. Marquet, J.-C. Merle, and J.-G. Gies, *Opt. Mater. (Amsterdam, Neth.)* **14**, 277 (2000).
- ¹¹Z.-Q. Fang and D. C. Look, *Appl. Phys. Lett.* **59**, 48 (1991).
- ¹²R. Chen, *Br. J. Appl. Phys., J. Phys. D* **2**, 371 (1969).
- ¹³A. Y. Polyakov, N. B. Smirnov, A. V. Govorkov, G. Dang, A. P. Zhang, F. Ren, X. A. Cao, S. J. Pearton, and R. G. Wilson, *J. Vac. Sci. Technol. B* **18**, 1237 (2000).